

## Binding kinetics of $^{11}\text{C}$ -*N*-methyl piperidyl benzilate ( $^{11}\text{C}$ -NMPB) in a rhesus monkey brain using the cerebellum as a reference region

Takashi ITOH,\* Masayasu TANAKA,\*\* Kaoru KOBAYASHI,\*\*\* Kazutoshi SUZUKI\*\* and Osamu INOUE\*\*\*

\*\*Center for Information and Sciences, Nippon Medical School

\*\*Department of Medical Imaging, National Institute of Radiological Sciences

\*\*\*School of Allied Health Sciences, Faculty of Medicine, Osaka University

The binding kinetics of  $^{11}\text{C}$ -*N*-methyl piperidyl benzilate ( $^{11}\text{C}$ -NMPB) in rhesus monkey brain were studied using animal positron emission tomography (PET) (SHR2000). This study is intended to assess the validity of the method using the cerebellum as a reference region, and to evaluate the effects of anesthesia on  $^{11}\text{C}$ -NMPB binding. Two monkeys, anesthetized with ketamine, received intravenous  $^{11}\text{C}$ -NMPB alone (370–760 MBq, <1  $\mu\text{g}/\text{kg}$ ) or mixed with varying doses of nonradioactive NMPB (3  $\mu\text{g}/\text{kg}$ , 10  $\mu\text{g}/\text{kg}$ , 30  $\mu\text{g}/\text{kg}$ ) and were subjected to PET scans for 60 minutes. Regions of interest (ROI) were drawn on reconstructed PET images and a time-activity curve was obtained for each region.  $^{11}\text{C}$ -NMPB accumulated densely in the striatum and cerebral cortex with time. In contrast, the tracer accumulation significantly decreased with increased doses of nonradioactive NMPB. In the cerebellum, on the other hand, the accumulation of  $^{11}\text{C}$ -NMPB remained low and the tracer was slowly eliminated from the brain following the injection.  $^{11}\text{C}$ -NMPB binding in the cerebellum was barely affected by the increased dose of nonradioactive NMPB. We thus concluded that the specific  $^{11}\text{C}$ -NMPB binding was negligible in the cerebellum, and performed simplified evaluation of  $^{11}\text{C}$ -NMPB binding in each brain region by a graphical method using the cerebellum as a reference region. PET was conducted 26 times, in total both in ketamine-anesthetized and awake monkeys ( $n = 3$  each). Measurements of  $^{11}\text{C}$ -NMPB binding showed good run-to-run reproducibility within individual animals. When  $^{11}\text{C}$ -NMPB binding was compared between ketamine-treated and awake animals, a significant increase in  $^{11}\text{C}$ -NMPB binding was observed in the striatum but not in other brain regions of ketamine-treated animals.

**Key words:**  $^{11}\text{C}$ -NMPB, rhesus monkey, cerebellum, reference region, conscious

### INTRODUCTION

MUSCARINIC ACETYLCHOLINE RECEPTORS (mAChR) are distributed with a high degree of density in the cerebral cortex, striatum and hippocampus and play important roles in numerous physiological functions such as motor function, temperature regulation, sleep, and memory.<sup>1–3</sup> Dysfunction of these receptors has been implicated in neurological disorders including dementia.<sup>4</sup>

Three pharmacologically distinct subclasses of mAChR,  $M_1$ – $M_3$ , have been identified<sup>5–7</sup>;  $M_1$  is predominant in the cortex while  $M_2$  is the major subclass in the cerebellum and heart.<sup>8,9</sup> 4-*N*-Methyl-piperidyl benzilate (NMPB) is a nonselective antagonist of the  $M_1$  and  $M_2$  receptors,<sup>10,11</sup> and the  $^3\text{H}$ - and  $^{11}\text{C}$ -ligands have been used for *in vivo* measurement of mAChR.<sup>12–14</sup>

In quantitative analysis of brain receptors by positron emission tomography (PET) or single photon emission computed tomography (SPECT), the distribution volume of radiolabeled ligands is typically measured using the fraction of free ligands in the blood and the kinetics of the ligands in the brain as the input and output functions, respectively.<sup>15</sup> However, for the analysis of dopamine receptors, the cerebellum serves as a reference region as

Received December 6, 2004, revision accepted July 27, 2005.

For reprint contact: Takashi Itoh, M.D., Center for Information and Sciences, Nippon Medical School, 1–1–5 Sendagi, Bunkyo-ku, Tokyo 113–8602, JAPAN.

E-mail: itoh@nms.ac.jp

it contains a minimal amount of dopamine receptors, and thus the time-activity curve (TAC) in the cerebellum is commonly used as the input function.<sup>16</sup>

The reference region method is noninvasive, does not require arterial blood sampling and allows easy relative quantification of receptors. This method has also been applied to the analysis of central benzodiazepine receptors (BZR) using <sup>11</sup>C-Ro15-1788, and brain regions with a relatively low BZR density, such as the pons, have been selected as a reference region.<sup>17</sup> Density of mAChR in the cerebellum has been reported to be very low both in rat<sup>18</sup> and monkey<sup>19</sup> as compared with these in the cortex. Thus, the cerebellum expressing low levels of mAChR may serve as a reference region in the quantitative analysis of mAChR by PET or SPECT. In the present study, we measured the kinetics of <sup>11</sup>C-NMPB binding in the cortex, striatum and cerebellum of rhesus monkeys and the effects of varying doses of nonradioactive ligands. As the cerebellum proved useful as a reference region, we further assessed run-to-run variations in <sup>11</sup>C-NMPB binding measurements and variations between ketamine-anesthetized and awake animals.

## MATERIALS AND METHODS

Male rhesus monkeys (6–9 kg) were anesthetized with ketamine (6 mg/kg) and fixed to a monkey chair.<sup>20</sup> Each monkey's head was fixed to the chair with a head-holder and positioned in the gantry of an animal PET scanner (SHR2000, Hamamatsu Photonics KK, Japan). This fixation system was designed to restrain the monkey's head only, allowing the limbs to move freely.

Two monkeys, deeply anesthetized with additional ketamine (5 mg/kg), received intravenous <sup>11</sup>C-NMPB alone (370–760 MBq, <1 μg/kg) or mixed with varying doses of nonradioactive NMPB (3 μg/kg, 10 μg/kg, 30 μg/kg). They were subjected to PET scans every minute for 60 minutes, starting 1 minute after <sup>11</sup>C-NMPB injection. <sup>11</sup>C-NMPB was produced by *N*-methylation of piperidyl benzilate using <sup>11</sup>C-methyl iodide<sup>21</sup> (radiochemical purity >98%, specific activity >37 GBq/μmol). Data were collected for seven slices simultaneously with a center-to-center distance of 8.0 mm. The horizontal resolution was 3.5 mm in the center of the field of view. Regions of interest (ROI) were drawn on reconstructed PET images and the TAC was obtained for each region.

As the second experiment, three monkeys were intravenously administered <sup>11</sup>C-NMPB alone under anesthesia with ketamine. Radioactivity in each brain region was measured as described above, and run-to-run reproducibility was assessed. The TAC of a reference region (cerebellum) and other brain regions (striatum and cortex) was obtained as the input and output functions, respectively, and <sup>11</sup>C-NMPB binding was analyzed by a graphical method (Patlak plot).<sup>22</sup> <sup>11</sup>C-NMPB binding kinetics in each brain region was also measured in three awake

monkeys for comparison with ketamine-anesthetized animals. <sup>11</sup>C-NMPB was injected after complete awaking (about 3 h after ketamine injection).

## RESULTS

Figure 1 shows accumulated images of PET scans after injection of <sup>11</sup>C-NMPB tracer alone. Figure 2 shows accumulated images taken over 60 minutes after injection of <sup>11</sup>C-NMPB mixed with varying doses of nonradioactive NMPB, and Figure 3 represents the TAC in the striatum, temporal cortex, occipital cortex, and cerebellum after injection of each <sup>11</sup>C-NMPB/NMPB dose.

When the animals received <sup>11</sup>C-NMPB alone, the radioactivity slowly accumulated in the striatum and cerebral cortex (temporal and occipital) with time, whereas in the cerebellum, the radioactivity remained low and reached a peak level after some minutes followed by a gradual decrease.

Accumulation of <sup>11</sup>C-NMPB in the striatum and cortex significantly decreased by increasing the dose of nonradioactive NMPB, but in the cerebellum, a slight decrease in tracer accumulation was noted only with 30 μg/kg NMPB. Furthermore, when 30 μg/kg NMPB was administered, the TAC in the striatum and cortex was similar to the TAC in the cerebellum, suggesting that mAChR was mostly saturated by the ligand.

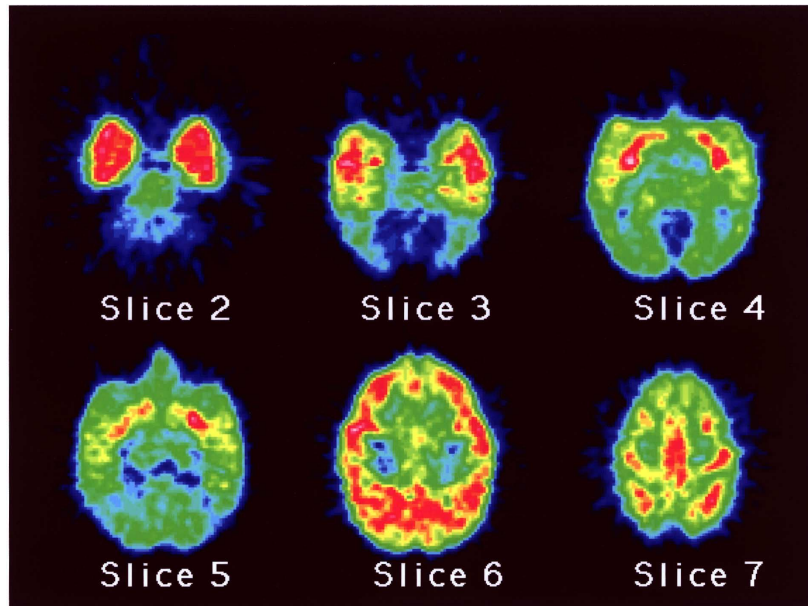
Figure 4 represents the Patlak plot of <sup>11</sup>C-NMPB binding in the striatum and cortex (temporal and occipital) using the TAC in the cerebellum as the input function. Good linear regression was observed in all examined regions.

Figure 5 (a) shows the binding index of <sup>11</sup>C-NMPB, as estimated by the graphical method in each brain region of the three monkeys anesthetized with ketamine. Four to five repetitive measurements performed for each monkey revealed small run-to-run variations, indicating good reproducibility of the <sup>11</sup>C-NMPB binding experiments. There were no significant variations either in the data among individual animals. <sup>11</sup>C-NMPB binding index in awake animals is shown in Figure 5 (b). No significant variations among measurements or individual animals were noted in the awake animals. When <sup>11</sup>C-NMPB binding was compared between awake and ketamine-anesthetized animals, ketamine treatment significantly increased the binding only in the striatum ( $p < 0.05$ ).

## DISCUSSION

When <sup>11</sup>C-NMPB was administered alone, radioactivity accumulated with time in the striatum and cortex, which are known to have high  $B_{\max}$  of mAChR. This indicates that the dissociation constant of the ligand-receptor complex is considered to approximate 0.

In the cerebellum, by contrast, radioactivity reached a peak level 5 minutes after injection, followed by a gradual



**Fig. 1** Accumulated PET images of rhesus monkeys taken over 60 minutes following injection of  $^{11}\text{C}$ -NMPB.

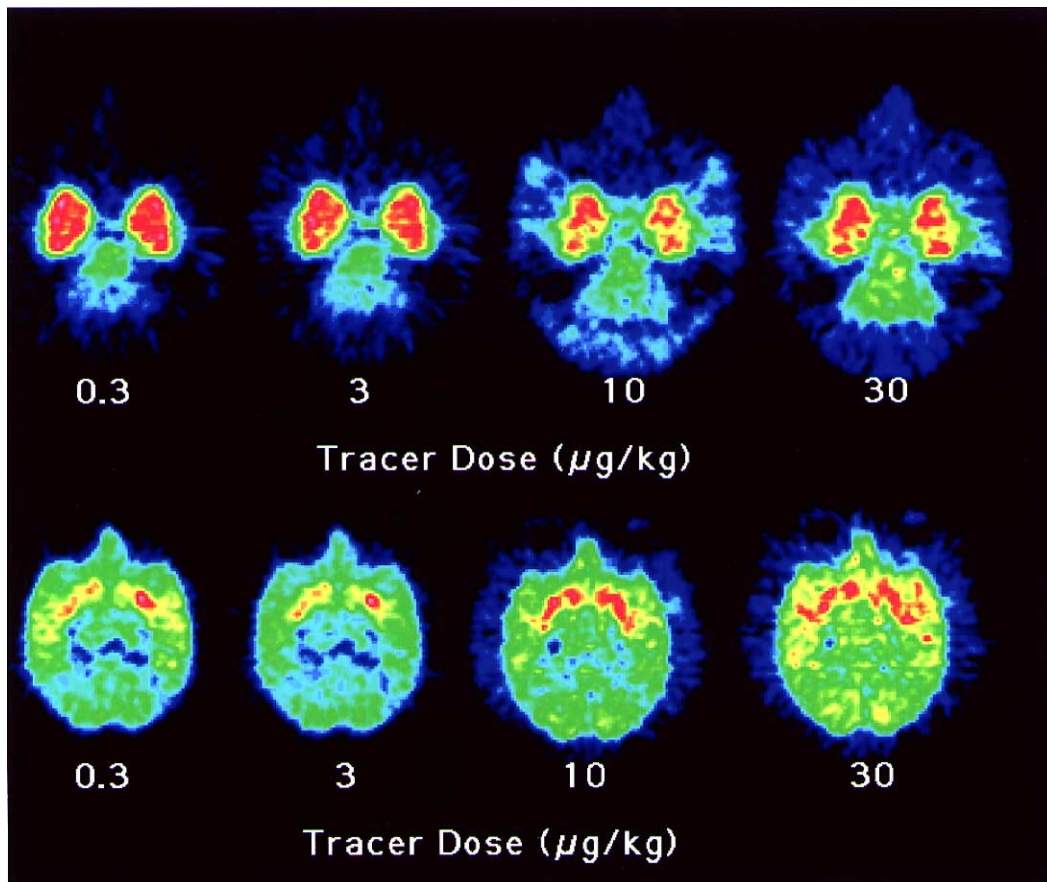


**Fig. 2** Accumulated PET images of the striatum and cerebellum of ketamine-anesthetized monkeys taken over 60 minutes following injection of  $^{11}\text{C}$ -NMPB mixed with varying doses of nonradioactive NMPB (0.3  $\mu\text{g}/\text{kg}$ , 3  $\mu\text{g}/\text{kg}$ , 10  $\mu\text{g}/\text{kg}$ , 30  $\mu\text{g}/\text{kg}$ ).

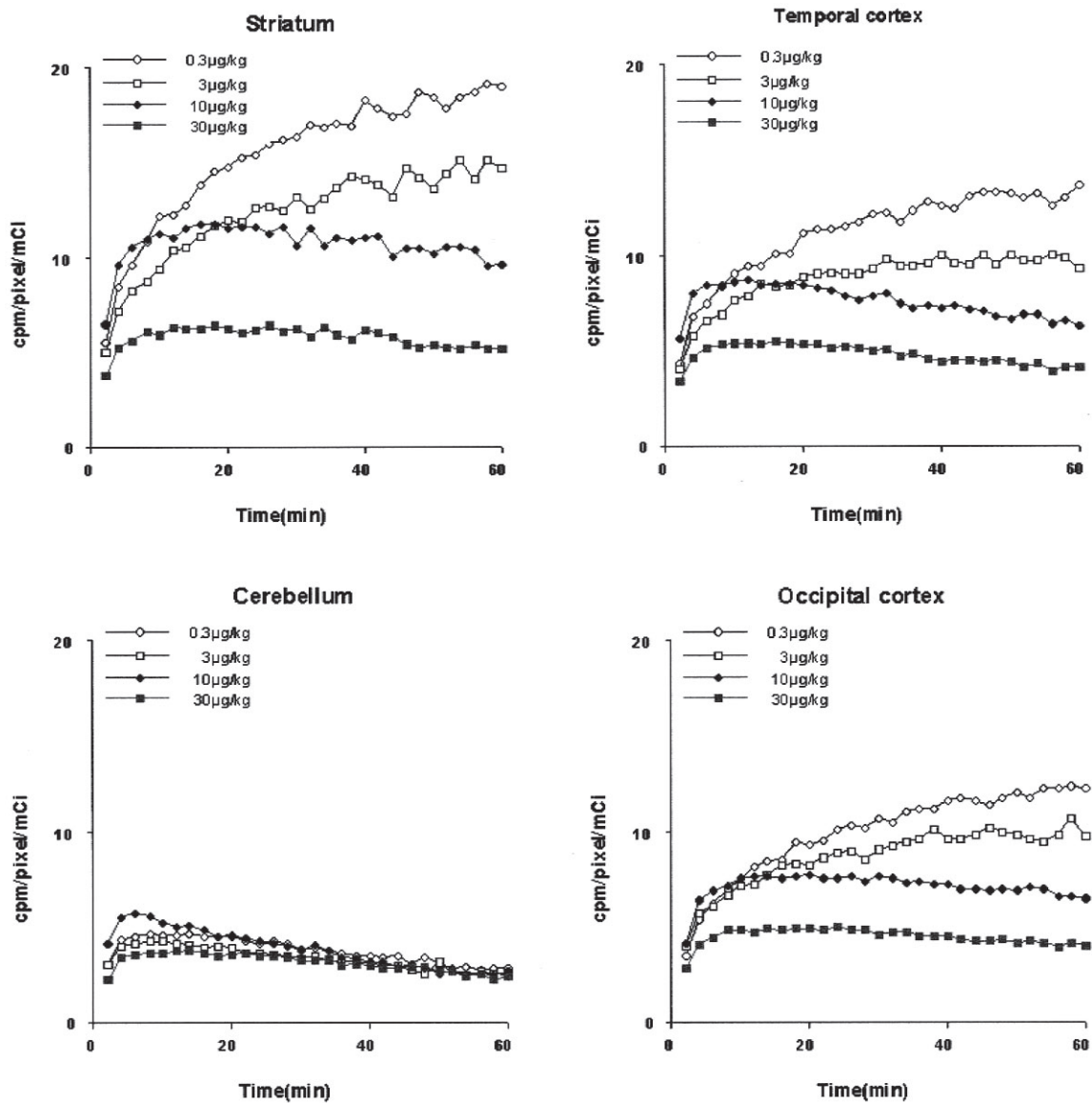


**Fig. 3** The TAC in the striatum, temporal cortex, occipital cortex, and cerebellum of ketamine-anesthetized monkeys after injection of  $^{11}\text{C}$ -NMPB mixed with varying doses of nonradioactive NMPB ( $0.3 \mu\text{g}/\text{kg}$ ,  $3 \mu\text{g}/\text{kg}$ ,  $10 \mu\text{g}/\text{kg}$ ,  $30 \mu\text{g}/\text{kg}$ ). Accumulation of  $^{11}\text{C}$ -NMPB in the striatum, temporal cortex and occipital cortex is decreased markedly by increasing the dose of nonradioactive NMPB. By contrast, tracer accumulation in the cerebellum is significantly lower compared to other regions and is minimally affected by increased doses of nonradioactive NMPB.

decrease in the activity. Accumulation of radioactivity at 60 minutes in the striatum, cortex, and cerebellum was approximately 19 count/pixel/mCi, 13 count/pixel/mCi, and 3 count/pixel/mCi, respectively, showing an extremely low level of accumulation in the cerebellum.

Miyoshi et al. reported the distribution of  $^3\text{H}$ -QNB binding and the  $M_1$  and  $M_2$  receptors in the monkey brain by *in vitro* autoradiography.<sup>19</sup> They showed that the  $B_{\text{max}}$  of  $^3\text{H}$ -QNB binding in the caudate nucleus and cerebellar cortex was 616 fmol/mg tissue and 36 fmol/mg tissue, respectively, indicating a significantly lower receptor density in the cerebellum (1/17) compared to the caudate

nucleus.  $^{11}\text{C}$ -NMPB, like  $^3\text{H}$ -QNB, is a subclass-nonspecific ligand, and its specific binding to mAChR *in vivo* is assumed to reflect the density of mAChR.

Tracer accumulation significantly decreased in the striatum and cortex by increasing the dose of nonradioactive NMPB, whereas only a small decrease in tracer accumulation was noted in the cerebellum, exhibiting virtually no differences among NMPB doses 60 minutes after administration. These findings suggest that competitive inhibition occurs in the striatum and cortex, which contain a large amount mAChR, whereas competitive inhibition is not apparent in the cerebellum. Thus, it is assumed that

$^{11}\text{C}$ -NMPB binding in the cerebellum contains only a limited amount of specific component.

The Patlak plot of  $^{11}\text{C}$ -NMPB binding in the striatum, temporal cortex and occipital cortex using the TAC in the cerebellum as the input function demonstrated good linear regression in each brain region, as shown in Figure 4. This study used the slope of these regression lines as a

relative binding index, although the slope contains a complex of binding parameters ( $K_1$ ,  $k_2$  and  $k_3$ ). Future research efforts should measure the arterial plasma free fraction as an input function for quantitative analysis using the compartment model. Analysis of binding in the equilibrium state was difficult because the dissociation rate of  $^{11}\text{C}$ -NMPB was very small. Tsukada et al. performed quantitative analysis of mAChR in conscious monkey brain using  $^{11}\text{C}$ -3-MPB, another radioligand.<sup>23,24</sup> The rank order of estimated binding potential (BP) of mAChR in various regions was consistent with our results. Because  $^{11}\text{C}$ -3-MPB has a lower relative affinity than  $^{11}\text{C}$ -NMPB,  $^{11}\text{C}$ -3-MPB seems to be a suitable tracer for quantitative analysis of mAChR.

Study of  $^{11}\text{C}$ -NMPB binding in brain regions of three monkeys under ketamine anesthesia (Fig. 5) revealed good reproducibility of measurements within the individual animal. Differences among the three monkeys were not significant either, demonstrating that the use of  $^{11}\text{C}$ -NMPB as a tracer allows estimation of mAChR binding. When  $^{11}\text{C}$ -NMPB binding was compared between awake and ketamine-anesthetized animals (Fig. 5), ketamine treatment significantly increased the binding only in the striatum in monkeys A and B ( $p < 0.05$ ), whereas a significant decrease in the binding was observed in all brain regions of awake monkey C.

It has been reported that the binding kinetics of a

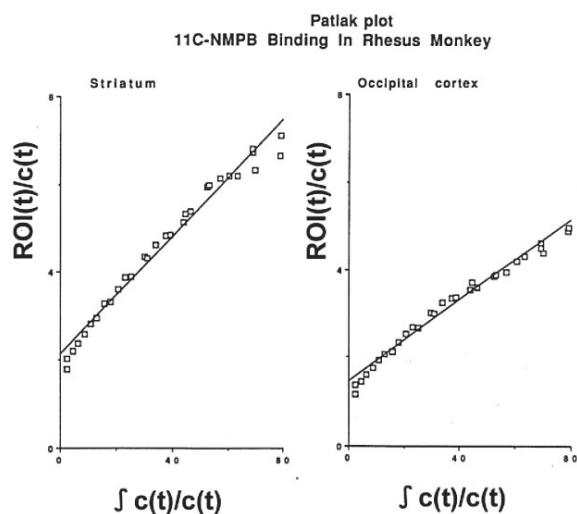


**Fig. 4** Patlak plots of  $^{11}\text{C}$ -NMPB binding in the striatum and cortex obtained using the TAC in the cerebellum as the input function.

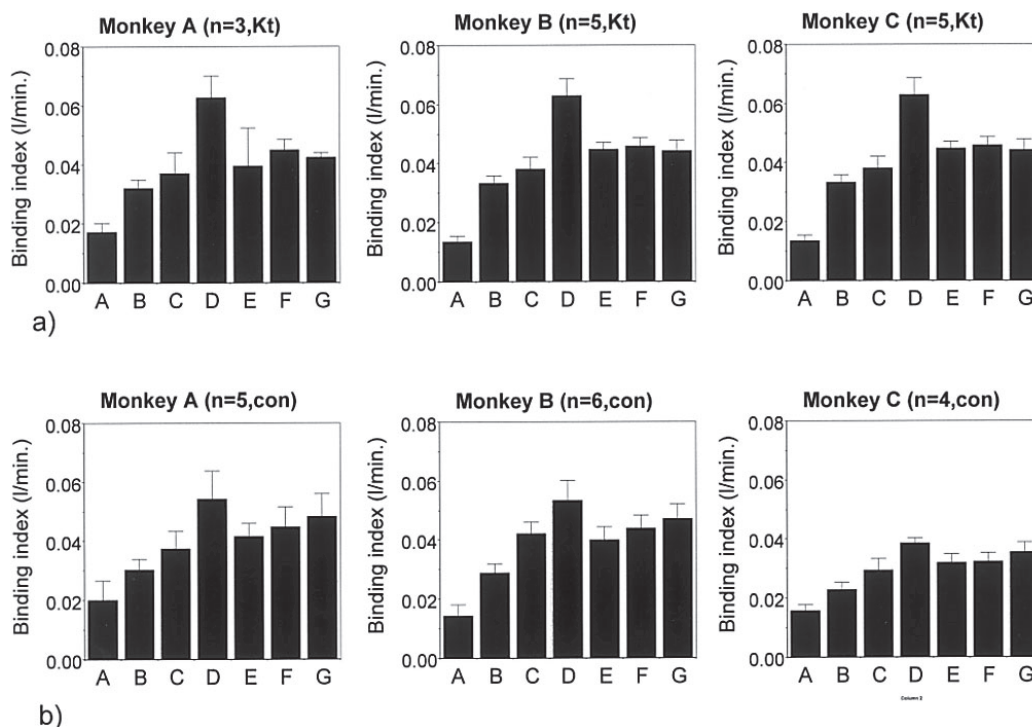


**Fig. 5** The  $^{11}\text{C}$ -NMPB binding index (the slope of Patlak plot) in each brain region of three monkeys (A, B and C), showing good run-to-run reproducibility. (a) Ketamine-anesthetized, ( $n = 3-5$ ). (b) Awaked, ( $n = 4-6$ ). A: Pons, B: Hippocampus, C: Thalamus, D: Striatum, E: Frontal cortex, F: Temporal cortex, G: Occipital cortex.

labeled ligand in the brain is significantly affected by the type of anesthetic drugs used. For example, the influence of anesthesia on  $^{11}\text{C}$ -raclopride binding in the monkey striatum varies significantly between ketamine and isoflurane, and isoflurane anesthesia significantly delays the binding/dissociation kinetics.<sup>25</sup> Compared to  $^{11}\text{C}$ -raclopride,  $^{11}\text{C}$ -NMPB binding was less significantly affected by ketamine anesthesia as shown in the present study. As ketamine has been reported to block *N*-methyl-D-aspartate (NMDA) receptors, the ketamine-induced increase in  $^{11}\text{C}$ -NMPB binding in the striatum may be mediated by NMDA receptors. Alternatively, ketamine has been shown to significantly increase the cerebral blood flow in rats,<sup>26</sup> and thus the apparent increase in  $^{11}\text{C}$ -NMPB binding in the striatum may be induced by increased cerebral blood flow, which enhances the delivery of the ligand from the blood into the brain. The tracer distribution patterns in monkeys A and B in the awake state were quite similar to those under ketamine anesthesia, whereas a decrease in  $^{11}\text{C}$ -NMPB binding in widespread brain regions was noted in monkey C when the animal was awake. As the monkeys were allowed to freely move their limbs during the measurements, the variations in  $^{11}\text{C}$ -NMPB binding between awake animals are considered to be baseline differences. In conclusion, the distribution of  $^{11}\text{C}$ -NMPB binding in the brain was consistent with the density distribution of mAChR, and showed good reproducibility at least in the ketamine-anesthetized and awake animals. Hence,  $^{11}\text{C}$ -NMPB was confirmed as a valid radiotracer for the PET analysis of mAChR.

## REFERENCES

1. Mitsui T. Acetylcholine receptor knockout mice. *Nihon Shinkei Seishin Yakurigaku Zasshi* 1999; 19: 233–238.
2. Bellingham MC, Ireland MF. Contribution of cholinergic systems to state-dependent modulation of respiratory control. *Respir Physiol Neurobiol* 2002; 131: 135–144.
3. Bartus RT, Dean RL 3rd, Beer B, Lippa AS. The cholinergic hypothesis of geriatric memory dysfunction. *Science* 1982; 217: 408–414.
4. Svensson AL, Alafuzoff I, Nordberg A. Characterization of muscarinic receptor subtypes in Alzheimer and control brain cortices by selective muscarinic antagonists. *Brain Res* 1992; 596: 142–148.
5. Hammer R, Berrie CP, Birdsall NJ, Burgen AS, Hulme EC. Pirenzepine distinguishes between different subclasses of muscarinic receptors. *Nature* 1980; 283: 90–92.
6. Doods HN, Mathy MJ, Davidesko D, van Charldorp KJ, de Jorge A, van Zwieten PA. Selectivity of muscarinic antagonists in radioligand and *in vivo* experiments for the putative M<sub>1</sub>, M<sub>2</sub> and M<sub>3</sub> receptors. *J Pharmacol Exp Ther* 1987; 242: 257–262.
7. Watson M, Roeske WR, Yamamura HI. [ $^3\text{H}$ ]pirenzepine and (-)-[ $^3\text{H}$ ]quinuclidinyl benzilate binding to rat cerebral cortical and cardiac muscarinic cholinergic sites. II. Characterization and regulation of antagonist binding to putative

- muscarinic subtypes. *J Pharmacol Exp Ther* 1986; 237: 419–427.
8. Luthin GR, Wolfe BB. Comparison of [ $^3\text{H}$ ]pirenzepine and [ $^3\text{H}$ ]zincuclidinylbenzilate binding to muscarinic cholinergic receptor in rat brain. *J Pharmacol Exp Ther* 1984; 228: 648–655.
9. Gibson RE, Moody T, Scineidau TA, Jagoda EM, Reba RC. The *in vitro* dissociation kinetics of (*R,R*)-[ $^{125}\text{I}$ ]4IQNB is reflected in the *in vivo* washout of the radioligand from rat brain. *Life Sci* 1992; 50: 629–637.
10. Klood Y, Egozi Y, Sokolovsky M. Characterization of muscarinic acetylcholine receptors from mouse brain: evidence for regional heterogeneity and isomerization. *Mol Pharmacol* 1979; 15: 545–558.
11. Klood Y, Egozi Y, Sokolovsky M. Regional heterogeneity of muscarinic receptors of mouse brain. *FEBS Lett* 1979; 97: 265–268.
12. Hosoi R, Kobayashi K, Watanabe Y, Inoue O. Evaluation of *in vivo* binding properties of  $^3\text{H}$ -NMPB and  $^3\text{H}$ -QNB in mouse brain. *J Neural Transm* 1999; 206: 583–592.
13. Suhara T, Inoue O, Kobayashi K, Suzuki K, Tateno Y. Age related changes in human muscarinic acetylcholine receptors measured by positron emission tomography. *Neurosci Lett* 1993; 149: 225–228.
14. Zubieta JK, Koeppe RA, Mulholland GK, Kuhl DE, Frey KA. Quantification of muscarinic cholinergic receptor with [ $^{11}\text{C}$ ]NMPB and positron emission tomography: method development and differentiation of tracer delivery from receptor binding. *J Cereb Blood Flow Metab* 1998; 18: 619–631.
15. Debruyne D, Abadie P, Barre L, Albessard F, Moulin M, Zarifian E, et al. Plasma pharmacokinetics and metabolism of the benzodiazepine antagonist [ $^{11}\text{C}$ ]Ro15-1788 (flumazenil) in baboon and human during positron emission tomography studies. *Eur J Drug Metab Pharmacokin* 1991; 16: 141–152.
16. Wong DF, Wanger HN Jr, Tune LE, Dannals RF, Perlson GD, Links JM, et al. Positron emission tomography reveals elevated D<sub>2</sub> dopamine receptors in drug-naïve schizophrenics. *Science* 1986; 234: 1558–1563.
17. Millet P, Graf C, Buck A, Walder B, Ibanez V. Evaluation of the reference tissue models for PET and SPECT benzodiazepine binding parameters. *Neuroimage* 2002; 17: 928–942.
18. Estevez EE, Jerusalinsky D, Medina JH, De Robertis E. Cholinergic muscarinic receptors in rat cerebral cortex, basal ganglia and cerebellum undergo rapid and reversible changes after acute stress. *Neuroscience* 1984; 13: 1353–1357.
19. Miyoshi R, Kito S, Shimoyama M. Quantitative autoradiographic localization of M<sub>1</sub> and M<sub>2</sub> subtypes of muscarinic acetylcholine receptors in monkey brain. *Jpn J Pharmacol* 1989; 51: 247–255.
20. Takechi H, Onoe H, Imamura K, Onoe K, Kakiuchi T, Nishiyama S, et al. Brain activation study by use of positron emission tomography in unanesthetized monkeys. *Neurosci Lett* 1994; 182: 279–282.
21. Suzuki K, Inoue O, Tamate K, Mikado F. Production of 3-*N*-[ $^{11}\text{C}$ ]methylspiperone with high specific activity and high radiochemical purity for PET studies: suppression of its radiolysis. *Int J Rad Appl Instrum [A]* 1990; 41: 593–599.

22. Patlak CS, Blasberg RG, Fenstermacher JD. Graphical evaluation of blood-to-brain transfer constants from multiple-time uptake data. *J Cereb Blood Flow Metab* 1983; 3: 1–7.
23. Tsukada H, Takahashi K, Miura S, Nishiyama S, Kakiuchi T, Ohba H, et al. Evaluation of novel PET ligands (+)N-[<sup>11</sup>C]methyl-3-piperidyl benzilate ([<sup>11</sup>C](+)3-MPB) and its stereoisomer [<sup>11</sup>C](–)3-MPB for muscarinic cholinergic receptors in the conscious monkey brain: a PET study in comparison with [<sup>11</sup>C]4-MPB. *Synapse* 2001; 39 (2): 182–192.
24. Tsukada H, Kakiuchi T, Nishiyama S, Ohba H, Sato K, Harada N, et al. Age differences in muscarinic cholinergic receptors assayed with (+)N-[<sup>11</sup>C]methyl-3-piperidyl benzilate in the brains of conscious monkeys. *Synapse* 2001; 41: 248–257.
25. Kobayashi K, Inoue O, Watanabe Y, Onoe H, Langstrom B. Difference in response of D<sub>2</sub> receptor binding between <sup>11</sup>C-N-methylspiperone and <sup>11</sup>C-raclopride against anesthetics in rhesus monkey brain. *L Neural Transm Gen Sect* 1995; 100: 147–151.
26. Burdett NG, Menon DK, Chapenter TA, Jones JG, Hall LD. Visualisation of changes in regional cerebral blood flow (rCBF) produced by ketamine using long TE gradient echo sequences: preliminary results. *Magn Reson Imaging* 1995; 13: 549–553.